Journal of Power Sources 195 (2010) 3031–3035

Contents lists available at ScienceDirect

Journal of Power Sources

journal homepage: www.elsevier.com/locate/jpowsour

Short communication

Electrophoretic deposition of graphene nanosheets on nickel foams for electrochemical capacitors

Yao Chen[a,b], Xiong Zhang[a], Peng Yu[a,b], Yanwei Ma[a,*]

[a] Institute of Electrical Engineering, Chinese Academy of Sciences, Beijing 100190, People's Republic of China
[b] Graduate University of Chinese Academy Sciences, Beijing 100049, People's Republic of China

ARTICLE INFO

Article history:
Received 31 August 2009
Accepted 13 November 2009
Available online 18 November 2009

Keywords:
Graphene nanosheets
Nickel foams
Electrochemical capacitors
Electrophoretic deposition

ABSTRACT

Graphene nanosheets are deposited on nickel foams with 3D porous structure by an electrophoretic deposition method using the colloids of graphene monolayers in ethanol as electrolytes. The high specific capacitance of 164 F g^{-1} is obtained from cyclic voltammetry measurement at a scan rate of 10 mV s^{-1}. When the current densities are set as 3 and 6 A g^{-1}, the specific capacitance values still reach 139 and 100 F g^{-1}, respectively. The high capacitance is attributed to nitrogen atoms in oxidation product of p-phenylene diamine (OPPD) adsorbed on the surface of the graphene nanosheets. The comparable results suggest potential application to electrochemical capacitors based on the graphene nanosheets.

1. Introduction

Electrochemical capacitors (ECs) are excellent electrical energy storage devices, exhibiting higher power density than rechargeable batteries and much greater capacitance than traditional dielectric capacitors [1]. With the unique advantages, ECs can be used either as the primary power sources independently or in combination with secondary cells to complement the low power density of them. Typically, they have great promise for potential applications such as mobile electronics, transportation, renewable energy production and aerospace systems [2]. Energy storage mechanisms of ECs are divided into two ways: double-layer capacitance and pseudocapacitance [3]. Commonly, porous carbon materials are the electrodes of double-layer capacitors, while transition metal oxides and conducting polymers are corresponding to pseudocapacitors [4]. Comparing with pseudocapacitors, more life time, lower cost and higher power density can be attained for double-layer capacitors. Hence carbonaceous materials with high specific area are the developed electrodes for ECs [5].

Graphene, which is discovered by Geim in 2004, is a 2D flat material consisting of monolayer carbon atoms [6]. As a new carbonaceous material, graphene has evident advantages for the applications in ECs because of its large theoretic specific surface area (2600 m^2 g^{-1}) and high room temperature electrical conductivity. Unlike activated carbon [7], the effective surface area of graphene does not depend on the distribution of pores but layers. Moreover the resistance of graphene is much smaller than that of activated carbon. Therefore graphene, especially chemically modified graphene which is prone to being produced on a large scale [8], is one of the most promising carbon materials to be applied to ECs. Recently, Vivekchand et al. [9] reported on graphene-based ECs, electrodes of which were prepared by thermal exfoliation, with the specific capacitance of 117 F g^{-1}. Stoller et al. [10] and Wang et al. [11] obtained the specific capacitance of 135 and 205 F g^{-1} at the current densities of 1.3 and 0.1 A g^{-1} by reducing graphite oxide with liquid and gas hydrazine hydrate, respectively.

In the process of fabricating electrodes, the choices of the current collectors and methods of depositing activated materials on them are the most crucial element to affect the performance of ECs. As one of the most economical and versatile methods for depositing films and coatings, electrophoretic deposition (EPD) enables the formation of high purity deposits of uniform thickness on substrates with complex shape [12,13]. With high demand on high surface area current collectors in ECs, porous nickel foams have particular advantages, such as 3D web containing the high accessible activated materials and better electrolytes access to activated materials to improve the electrochemical performance [14,15].

More recently, another strategy of preparing graphene and graphene films has been exploited by our group. We have fabricated the stable graphene colloids by reducing exfoliated graphite oxide with p-phenylene diamine [16]. Considering the graphene nanosheets are positively charged due to adsorbing the oxidation product of p-phenylene diamine (OPPD) with –N$^+$, we devel-

* Corresponding author at: Tel.: +86 10 82547129; fax: +86 10 82547137.
E-mail address: ywma@mail.iee.ac.cn (Y. Ma).

0378-7753/$ – see front matter © 2009 Elsevier B.V. All rights reserved.
doi:10.1016/j.jpowsour.2009.11.057

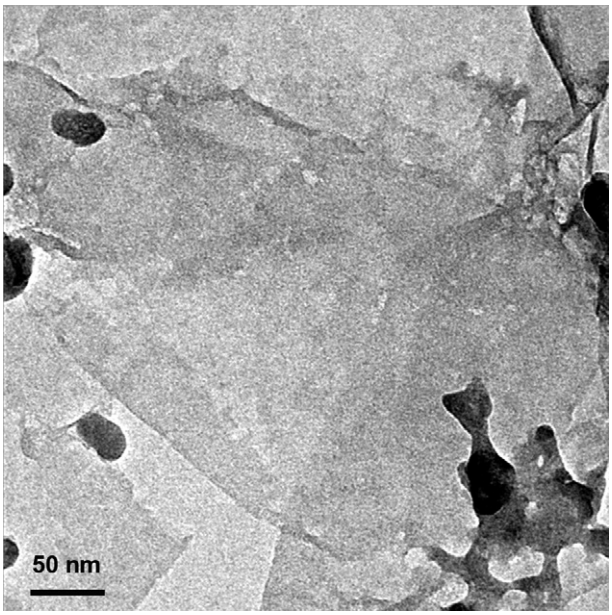

Fig. 1. TEM image of graphene nanosheets dispersed in ethanol.

oped the EPD method to deposit graphene on the nickel foams as electrodes of ECs. The high specific capacitance of 164 F g^{-1} is obtained from cyclic voltammetry measurement at a scan rate of 10 mV s^{-1}.

2. Experimental

Stable graphene colloids modified by OPPD were synthesized according to the literature [16]. The as-made graphene was filtered and washed with acetone. Then the washed graphene powders were transferred into ethanol to form stable graphene colloids after mild ultrasonication with an approximate concentration of 0.1 mg mL^{-1}. The course of the EPD was as follows: a piece of nickel foam was used as the negative electrode and indium tin oxide (ITO)-coated conductive glass as the positive electrode; the graphene colloids in ethanol were electrolyte. The distance between the two electrodes was 1 cm and the applied voltage was 50 V. After deposition, the graphene sheets on the nickel foams were annealed at 400 °C for 3 h under the flow of Ar.

The transmission electron microscopy (TEM) images of graphene colloids were investigated by JEOL JSM 2010. The field emission scanning electron microscopy (FESEM) images of the nickel foams before and after EPD were observed by JEOL JSM 6700F. The electrode performance was measured in a beaker-type electrochemical cell with the graphene sheets on nickel foam after deposition and annealing as a work electrode, a platinum counter electrode and a standard Hg/HgO electrode as a reference one. The electrolyte was 6 M KOH aqueous solution. Cyclic voltammetry scans were recorded from −0.8 to 0 V (vs. Hg/HgO) at different scan rates. Galvanostatic charge/discharge cycling in the potential range of −0.6 to 0 V was performed at different constant current densities. Both the two electrochemical methods were carried out with CHI 660C workstation.

3. Results and discussion

In our previous studies, colloids of graphene monolayers in ethanol had been demonstrated by atomic force microscope (AFM) and X-ray photoelectron spectroscope (XPS) [16]. Fig. 1 shows the TEM images of graphene sheets dispersed in ethanol. The nanoscale graphene sheets are very thin with some black dots, which have been confirmed to be OPPD, covering on the surface of the graphene sheets. It is found that the stable graphene colloids can remain for a long time. Obviously, the residual OPPD is a good dispersant for graphene. Moreover, it made graphene nanosheets positively charged, being convenient for the applications of EPD. ITO-coated glass was used as the substrate on which graphene nanosheets were deposited by EPD [16]. However, the conductivity of ITO is small and the graphene may be exfoliated from the ITO in the electrolyte under the electrochemical reactions. So porous nickel foams are much more suitable than ITOs as current collectors. Fig. 2b shows the morphology of the graphene nanosheets deposited on the nickel foam, comparing with that of bare nickel foam with a 3D cross-linked grid structure (Fig. 2a). There is no obvious difference between them via low magnification FESEM views. Thus middle and high magnification images need to be studied. There are black coatings on the nickel foam treated by EPD in Fig. 2d, while nothing can be observed on the bare nickel foam (Fig. 2c). In Fig. 2e, black graphene nanosheets on the white nickel substrate can be observed from the high magnification image. Evidently, some corrugation and scrolling are clear on the surface of the graphene coatings, suggesting that some graphene nanosheets may aggregate after EPD. The thin and flat coatings may correspond to few layers of graphene.

Fig. 3 shows the cyclic voltammetry (CV) profiles of the graphene nanosheets electrode at different scan rates and a bare nickel foam at 10 mV s^{-1} in a potential range between −0.8 and 0 V. In the case of 100 mV s^{-1}, a nonrectangular shape was observed. Clearly enhanced capacitance can be attributed to adsorption/desorption of positively charged ions in negative potentials. Considering that the graphene contained 10% of nitrogen according to the prevenient XPS result, the deviation from the imaginary rectangle may be caused by pseudocapacitive effects between potassium cations and the nitrogen atoms of graphene [17]. While the CV of the bare nickel foam at 10 mV s^{-1} is negligible when compared with the graphene nanosheets electrode at the same condition. The specific capacitance of the graphene nanosheets electrode is calculated using the integrated area of charge curve which is more accurate than the half one of the full CV curve. Concretely, the former, which is smaller than the latter, is obtained based on Eq. (1):

$$C = \frac{1}{\Delta V \cdot m \cdot s} \int_{-0.8\,\mathrm{V}}^{0\,\mathrm{V}} |i| dV \quad (1)$$

where ΔV is the potential window, m is the mass of the graphene nanosheets, s is the scan rate, i is the instantaneous charge current in given potential. In order to expel the contribution of nickel foam to the specific capacitance, integrated area of curve (d) in Fig. 3 should be subtracted. The specific capacitance values at 10 mV s^{-1} before and after subtracting that of the bare nickel foam are both 164 F g^{-1}. So the CV curves of the graphene nanosheets electrode reflect the behavior of the graphene nanosheets without the effect of nickel.

The capacitance retention ratio of the graphene, 60% at 100 mV s^{-1} which corresponds to 97 F g^{-1}, is shown in Fig. 4. Also, the retention ratios of it at 20 and 50 mV s^{-1} are 89 and 73%, respectively. The ratio is smaller than other reports [10,18] due to low normal conductivity [19] of the graphene nanosheets absorbing OPPD. In addition, graphene sheets have no pores to provide a short ion-transport pathway in normal plane so that an electric double layer can only form at the surface of it in a short time, which may decrease the retention ratio of the graphene nanosheets electrode. The cycle performance of the graphene nanosheets electrode was

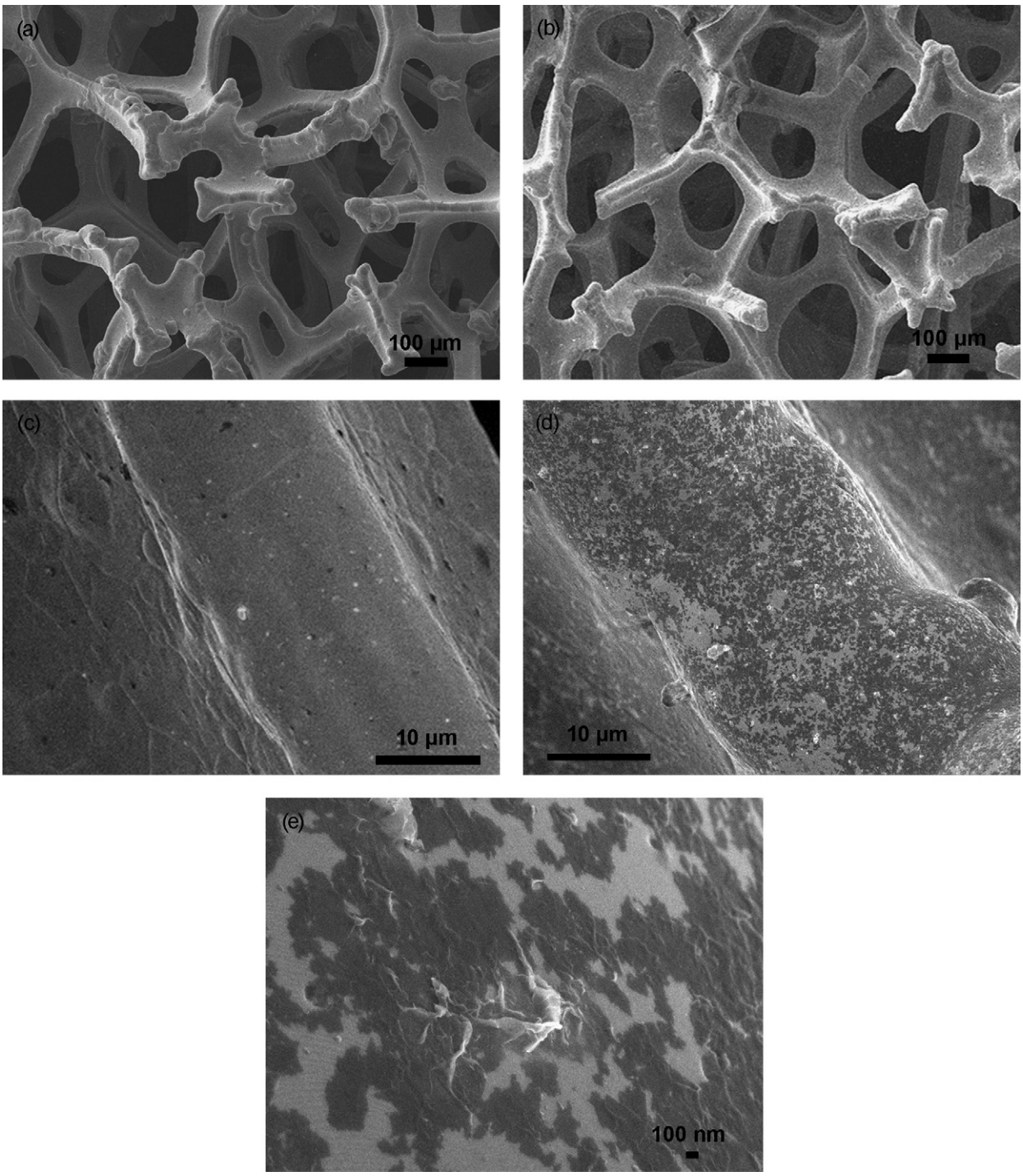

Fig. 2. FESEM images of (a) and (c) bare nickel foam and (b), (d) and (e) graphene nanosheets deposited on nickel foam.

elucidated by CV. From Fig. 5, it is noticed that repetitive measurements at 5 mV s^{-1} result in charged specific capacitance loss. Fig. 6 exhibits the cycle life data of the graphene nanosheets. With increasing the cycle numbers, the specific capacitance decreases. After 700 cycles, the specific capacitance remains 61% of the maximum capacitance.

Fig. 7 shows the results of galvanostatic charge/discharge cycling at high current densities of 3 and 6 A g^{-1}. The specific capacitance values are 139 and 100 F g^{-1}, respectively. The high specific capacitance even at a relative high current density may be attributed to the nitrogen atoms of OPPD doped in graphene matrix [20]. The chargeable nitrogen at the periphery of the graphene layers can adsorb more charges from the electrolyte and improve the charge-exchange characteristics of carbon [21]. The modification of surface polarity of graphene nanosheets with nitrogen can not only strengthen the wettability of the interface between electrode and electrolyte, but also introduce pseudocapacitive effects [22,23].

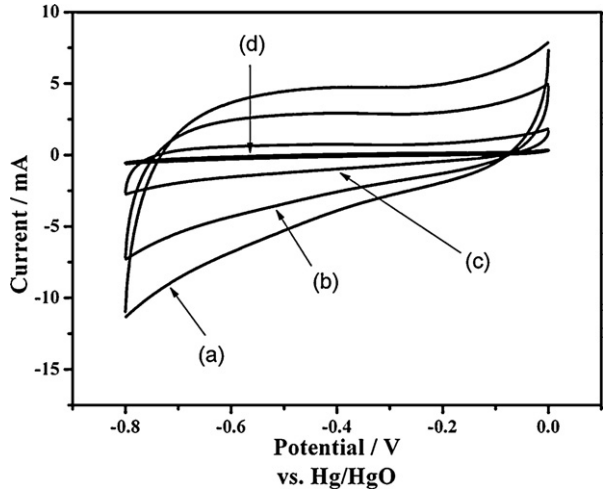

Fig. 3. CVs of the graphene nanosheets electrode at scan rates of (a) 100, (b) 50, (c) 10 mv s^{-1} and (d) bare nickel foam electrode at 10 mv s^{-1} in 6 M KOH within the potential range: −0.8 to 0 V (vs. Hg/HgO).

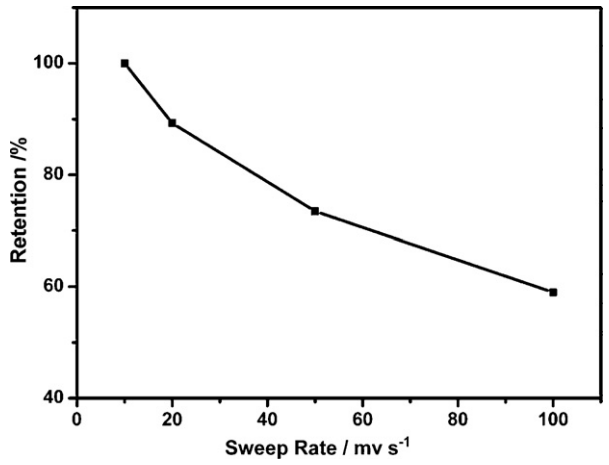

Fig. 4. Capacitance retention ratio as a function of the potential scan rate.

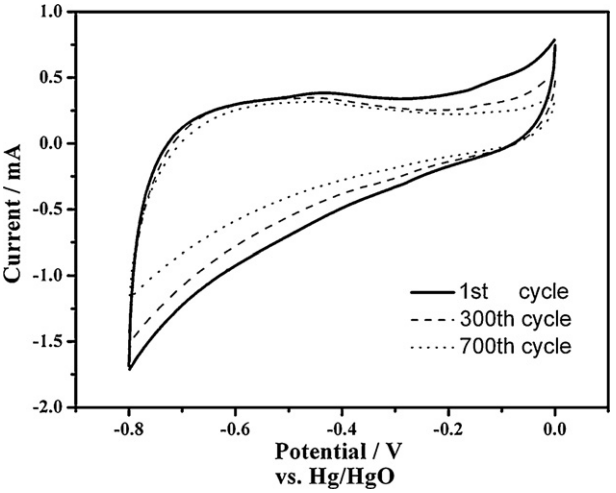

Fig. 5. CV of the graphene nanosheets electrode after 1, 300 and 700 cycles at 5 mV s^{-1}.

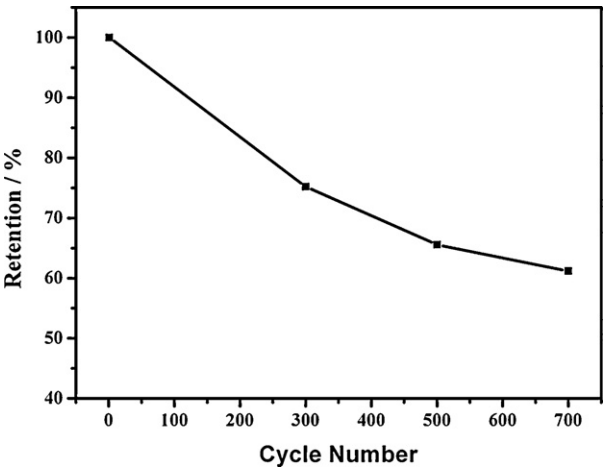

Fig. 6. Cyclic performances of the graphene nanosheets electrode.

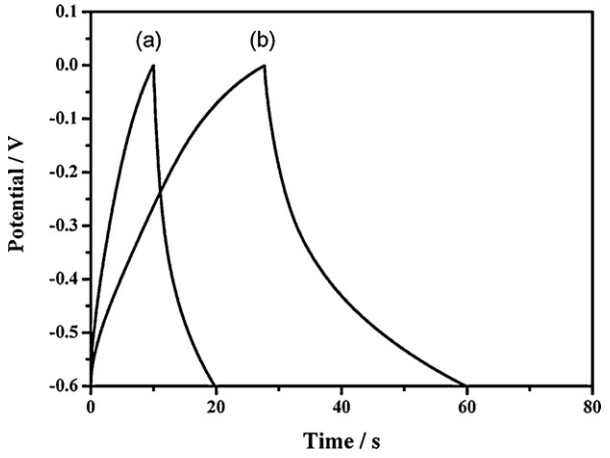

Fig. 7. Charge/discharge curves of the graphene nanosheets electrode at current densities of (a) 6 A g^{-1} and (b) 3 A g^{-1}.

4. Conclusion

We have employed an electrophoretic deposition method to make the graphene nanosheets on nickel foam as the electrode of ECs. Both corrugation and flat thin nanosheets exist in the graphene coatings we prepared via FESEM observations. High specific capacitance of 164 F g^{-1} is achieved from CV at a scan rate of 10 mV s^{-1}. At high current density of 3 and 6 A g^{-1}, the specific capacitance values still reach 139 and 100 F g^{-1}, respectively. The nitrogen doped in graphene nanosheets can not only strengthen the wettability of the interface between electrode and electrolyte, but also introduce pseudocapacitive effects. The graphene shows the good application potential in ECs. In next studies, the retention ratio of the graphene nanosheets electrode need be enhanced further by increasing the normal conductivity of the graphene nanosheets.

Acknowledgements

This work was partially supported by the Knowledge Innovation Program of the Chinese Academy of Sciences (No. KJCX2-YW-W26), the National Natural Science Foundation of China (No. 50802093) and the Director Foundation of Institute of Electrical Engineering..

References

[1] J.-W. Lang, L.-B. Kong, W.-J. Wu, Y.-C. Luo, L. Kang, Chem. Commun. (2008) 4213–4215.

[2] P. Simon, Y. Gogotsi, Nat. Mater. 7 (2008) 845–854.
[3] K.-W. Nam, K.-B. Kim, J. Electrochem. Soc. 149 (2002) A346–A354.
[4] A.G. Pandolfo, A.F. Hollenkamp, J. Power Sources 157 (2006) 11–27.
[5] D. Yuan, J. Chen, J. Zeng, S. Tan, Electrochem. Commun. 10 (2008) 1067–1070.
[6] K.S. Novoselov, A.K. Geim, S.V. Morozov, D. Jiang, Y. Zhang, S.V. Dubonos, I.V. Grigorieva, A.A. Firsov, Science 306 (2004) 666–669.
[7] G. Lota, T.A. Centeno, E. Frackowiak, F. Stoeckli, Electrochim. Acta 53 (2008) 2210–2216.
[8] M. Choucair, P. Thordarson, J.A. Stride, Nat. Nanotechnol. 4 (2009).
[9] S.R.C. Vivekchand, C.S. Rout, K.S. Subrahmanyam, A. Govindaraj, C.N.R. Rao, J. Chem. Sci. 120 (2008) 9–13.
[10] M.D. Stoller, S. Park, Y. Zhu, J. An, R.S. Ruoff, Nano Lett. 8 (2008) 3498–3502.
[11] Y. Wang, Z. Shi, Y. Huang, Y. Ma, C. Wang, M. Chen, Y. Chen, J. Phys. Chem. C 113 (2009) 13103–13107.
[12] Z.-S. Wu, S. Pei, W. Ren, D. Tang, L. Gao, B. Liu, F. Li, C. Liu, H.-M. Cheng, Adv. Mater. 21 (2009) 1756–1760.
[13] X. Fan, W. Peng, Y. Li, X. Li, S. Wang, G. Zhang, F. Zhang, Adv. Mater. 20 (2008) 4490–4493.
[14] J. Li, Q.M. Yang, I. Zhitomirskya, J. Power Sources 185 (2008) 1569–1574.
[15] G.-W. Yang, C.-L. Xu, H.-L. Li, Chem. Commun. (2008) 6537–6539.
[16] Y. Chen, X. Zhang, P. Yu, Y. Ma, Chem. Commun. (2009) 4527–4529.
[17] D. Hulicova, M. Kodama, H. Hatori, Chem. Mater. 18 (2006) 2318–2326.
[18] D.-W. Wang, F. Li, M. Liu, G.Q. Lu, H.-M. Cheng, Angew. Chem. Int. Ed. 47 (2008) 373–376.
[19] C.-W. Huang, C.-M. Chuang, J.-M. Ting, H. Teng, J. Power Sources 183 (2008) 406–410.
[20] W. Kim, J.B. Joo, N. Kim, S. Oh, P. Kim, J. Yi, Carbon 47 (2009) 1407–1411.
[21] N.D. Kim, W. Kim, J.B. Joo, S. Oh, P. Kim, Y. Kim, J. Yi, J. Power Sources 180 (2008) 671–675.
[22] H. Guo, Q. Gao, J. Power Sources 186 (2009) 551–556.
[23] W. Li, D. Chen, Z. Li, Y. Shi, Y. Wan, J. Huang, J. Yang, D. Zhao, Z. Jiang, Electrochem. Commun. 9 (2007) 569–573.